Cyclization Mechanism of Amorpha-4,11-diene Synthase, a Key Enzyme in Artemisinin Biosynthesis

Soon-Hee Kim,[†] Keon Heo,[‡] Yung-Jin Chang,[†] Si-Hyung Park,[§] Sang-Ki Rhee,[†] and Soo-Un Kim*[,†,⊥]

School of Agricultural Biotechnology, Seoul National University, Seoul 151-921, Korea, Research and Development Center, Doosan Cooperation, Yongin 449-795, Korea, Department of Pharmacognostic Resources, Mokpo National University, Muan 534-729, Korea, and Plant Metabolism Research Center, Kyung Hee University, Yongin 449-701, Korea

Received September 22, 2005

Cyclization of farnesyl diphosphate into amorpha-4,11-diene by amorpha-4,11-diene synthase (ADS) initiates biosynthesis of artemisinin, a clinically important antimalarial drug precursor. Three possible ring-closure mechanisms, two involving a bisabolyl carbocation intermediate followed by either a 1,3-hydride shift or two successive 1,2-shifts, and one involving a germacrenyl carbocation, were proposed and tested by analyzing the fate of farnesyl diphosphate H-1 hydrogen atoms through ^{1}H and ^{2}H NMR spectroscopy. Migration of one deuterium atom of [1,1-$^{2}H_2$]farnesyl diphosphate to H-10 of amorpha-4,11-diene singled out the bisabolyl carbocation mechanism with a 1,3-hydride shift. Further confirmation was obtained through enzyme reactions with (1*R*)- and (1*S*)-[1-^{2}H]farnesyl diphosphate. Results showed that deuterium of the 1*R* compound remained at H-6, whereas that of the 1*S* compound migrated to H-10 of amorpha-4,11-diene. Incorporation of one deuterium into amorphadiene in the cyclization process was observed when the reaction was performed in $^{2}H_2O$, as evidenced by an increase of 1 amu in the mass of the molecular ion.

The importance of terpenoids in human health care can never be overemphasized, as evidenced by terpenoid-derived drugs such as paclitaxel. The role of terpenoids in chemical communication between species is also an important factor in ecology. In this regard, the chemistry and biology of terpene biosynthesis have been receiving much scientific and biotechnological attention. The recent discovery of the 2-C-methyl-D-erythritol-4-phospahte (MEP) pathway in bacteria[1,2] and plants[3] offers new opportunities to understand and manipulate the biosynthesis of these vital molecules. Cloning of terpene cyclases from various sources, on the other hand, enabled us to gain deeper insight into the molecular action and biology of terpene biosynthesis.[4] In particular, the availability of large amounts of the cyclase produced by heterologous expression in *E. coli* offered an opportunity to directly probe the action mechanism of the enzyme. Long before the unraveling of the three-dimensional structures of terpene cyclases, various methods had been employed to probe the cyclization process. For example, the use of deuterium-labeled substrates enabled researchers to study the mechanism by observing the labeling pattern of the enzymatic product.[5−7] Labeled substrate was also used to help identify the intermediate carbocation during cyclization. Recently, elucidation of the three-dimensional structure of *epi*-aristolochene synthase from tobacco (TEAS) opened a new avenue into explaining the enzyme action in a more detailed manner with respect to the putative mechanism.[8]

Amorpha-4,11-diene synthase (ADS) of *Artemisia annua* L. is a sesquiterpene cyclase that catalyzes the conversion of farnesyl diphosphate into amorpha-4,11-diene in the biosynthesis of artemisinin, a precursor of the clinically important antimalarial drug artesunate.[9] There has been intense interest in the unraveling of the biosynthetic pathway leading to artemisinin and cloning of the involved enzymes. The knowledge gained through these studies could be directly applied to engineering of the plant toward higher artemisinin production. A cDNA coding ADS, the only enzyme so far identified to operate in the biosynthesis of artemisinin, was cloned from *A. annua* and functionally identified through expression in *E. coli.*[10] The enzyme produces an amorphane-type ring, whereas δ-cadinene synthase (CDS) in cotton[11] makes the same carbon skeleton but with a configuration and double bond geometry different from those of amorpha-4,11-diene. Therefore, unraveling the action mechanism of ADS would enable us to understand the requirements involved in the bifurcation of the catalytic pathway into the δ-cadinane or amorphadiene skeleton.

In the biosynthesis of amorpha-4,11-diene by ADS, two mechanisms involving a bisabolyl cation from the initial 1,6-closure (pathways a and b, Figure 1) and one involving a germacryl cation from the initial 1,10-closure (pathway c, Figure 1) are possible. Among the bicyclic sesquiterpene synthases, CDS,[11] TEAS,[12] and pentalenene synthase[13] are known to produce a germacryl cation as the initial cyclic intermediate. This prevalence of the germacryl intermediate in the cyclase catalysis prompted us to consider the viability of pathway c as an ADS action mechanism. However, Picaud et al. proposed that ADS catalysis proceeds through the bisabolyl intermediate (pathway a), a conclusion based on the appearance of the reaction byproducts with a bisabolane skeleton.[14] Alternatively, if one considers successive 1,2-hydride shifts instead of one 1,3-hydride shift before the second annulation, a variant bisabolyl mechanism (pathway b, Figure 1) would be possible. Recently during manuscript preparation, Brodelius' group arrived at the conclusion that ADS catalyzes initial 1,6-ring closure followed by a stereospecific 1,3-hydride shift based on the indirect observation of ^{2}H by ^{1}H NMR in amorpha-4,11-diene derived from deuterium-labeled FPP.[15]

The present research was performed to establish the mechanism of the ADS reaction by determining the migration of farnesyl diphosphate H-1 atoms, in a different manner from Brodelius' group, in the cyclization process. In this work, the deuterium-labeled product amorpha-4,11-diene was analyzed by ^{2}H NMR to locate the position of the label. On the basis of these observations, we confirmed the operation of a bisabolyl mechanism involving one 1,3-hydride shift (pathway a), and a mechanism explaining the observed deuterium exchange with the medium was postulated.

Results and Discussion

Protein Purification. The recombinant ADS protein tagged with His_6 was purified through a single-step nickel column chromatography. The eluent was monitored by SDS-PAGE (Supporting Information), and the purified enzyme with a MW of 61 was used

* To whom correspondence should be addressed. Tel: 82-2-880-4642. E-mail: soounkim@plaza.snu.ac.kr.
[†] School of Agricultural Biotechnology, SNU.
[‡] Doosan Cooperation.
[§] Department of Pharmacognostic Resources, MNU.
[⊥] Plant Metabolism Research Center, KHU.

10.1021/np050356u CCC: $33.50
Published on Web 05/26/2006

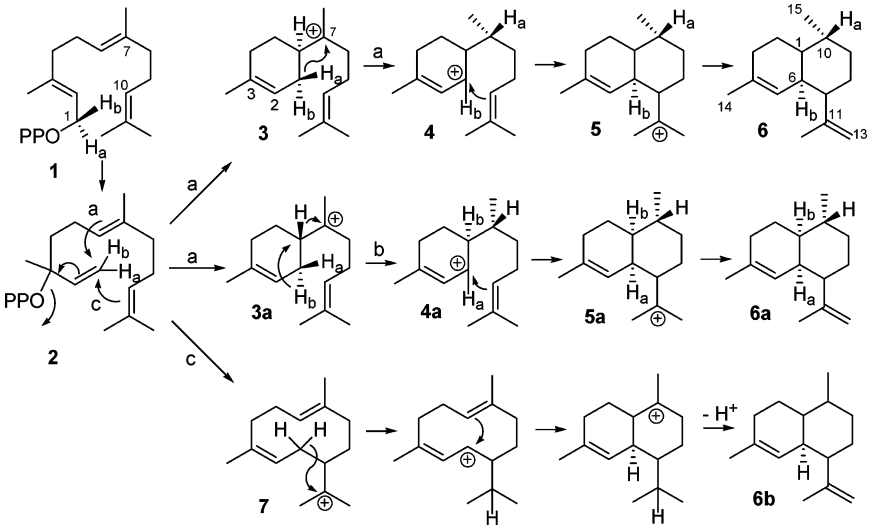

Figure 1. Three possible mechanisms of ADS action. Pathways a and b involve one 1,3- and two 1,2-hydride shifts, respectively, after the initial formation of a bisabolyl cation intermediate through 1,6-ring closure. Pathway c is characterized by initial formation of a germacryl carbocation intermediate arising from 1,10-ring closure.

in the reaction with farnesyl diphosphate. The purity of the enzyme used in the preparative reaction was estimated to be >95% by SDS-PAGE.

Synthesis of Deuterium-Labeled Farnesyl Diphospahtes. Asymmetric labeling at H-1 of farnesyl diphosphate was achieved through the reduction of [1-^{2}H]farnesal with (*R*)- or (*S*)-alpine borane.[17] To avoid ambiguity in the interpretation of amorphadiene spectra, deuterium labeling of farnesyl diphosphate with high enantiomeric purity was required at H-1. The reported enantiopurity of [1-^{3}H]isopentenyl diphosphate similarly prepared is 98% ee.[18] The presence of the diphosphate group in the final products was confirmed by ^{31}P NMR (data not shown), and the resulting farnesyl diphosphates were used as ammonium salts.

Position of Deuterium Label. Incubations were performed under the established 1 mL assay condition to ensure high conversion of farnesyl diphosphate into amorphadiene. Enzymatic cyclization with the unlabeled substrate afforded amorphadiene (>95%) and some byproducts, as shown by gas chromatography analysis (Supporting Information).

Inspection of the mass fragmentation patterns (Supporting Information) revealed the presence of deuterium in all labeled amorpha-4,11-diene samples. Labeled amorphadiene obtained through the incubation of singly and doubly labeled farnesyl diphosphates yielded molecular ions at *m*/*z* 205 and 206, respectively. No significant differences were observed in the mass spectra of H-6 and H-10 labeled amorphadienes. The deuterium position was elucidated by ^{2}H NMR (Figure 2) and also by ^{1}H NMR (Figure 3) as follows. The chemical shift value of deuterium is, in general, identical to the corresponding proton chemical shift; therefore, this chemical shift relationship was used to observe the ^{2}H label during the cyclization of farnesyl diphosphate by ADS. Due to the low intrinsic magnetic sensitivity of ^{2}H nuclei and small sample quantities, attaining a high signal-to-noise ratio value was difficult, especially in the singly labeled compounds. As a compromise between the magnetic field stability and measuring time, a signal-to-noise ratio of 1.8, which was just adequate for positively judging the presence of ^{2}H, even in the least concentrated sample, was adopted (Figure 2C). The amorphadiene derived from [1,1-$^2H_2$]-farnesyl diphosphate displayed signals at δ 1.38 and 2.60 (Figure 2A), corresponding to the proton signals of H-10 and H-6 at δ 1.40 and 2.55, respectively. Broadening of the peak, unavoidable due to the quadrupolar nature of the ^{2}H nucleus and field drift during the long accumulation period, resulted in chemical shifts slightly different from those observed in the ^{1}H NMR spectrum. Intensities

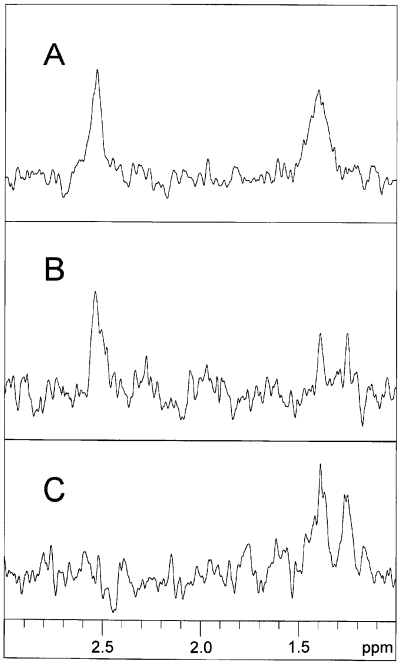

Figure 2. ^{2}H NMR spectra of amorphadienes: (A) from [1,1-$^2H_2$]-farnesyl diphosphate; (B) from (1*R*)-[1-^{2}H]farnesyl diphosphate; (C) from (1*S*)-[1-^{2}H]farnesyl diphosphate.

of the signals were comparable, indicating the presence of one deuterium at each site.

To ascertain which deuterium of [1,1-$^2H_2$]farnesyl diphosphate migrated to H-10 of amorphadiene, [1-^{2}H]farnesyl diphosphates asymmetrically labeled at H-1 were prepared. Incubation of (1*R*)-[1-^{2}H]farnesyl diphosphate with ADS yielded a singly labeled product, whose ^{2}H NMR signal appeared at δ 2.60 (Figure 2B). This sample had small signals at δ 1.38 and 1.25, the former possibly due to the incomplete induction of asymmetry on C-1 of the labeled farnesyl diphosphate sample and the latter due to impurity. The 1*S* isomer gave rise to amorphadiene with a signal at δ 1.38. Again, the sample had an impurity signal at δ 1.25 (Figure 2C).

The position of the deuterium label in amorphadiene was confirmed by ^{1}H NMR measurement. The ^{1}H spectrum of amorphadiene from doubly labeled farnesyl diphosphate lacked signals at both δ 1.40 and 2.55 as expected (Figure 3B), confirming the

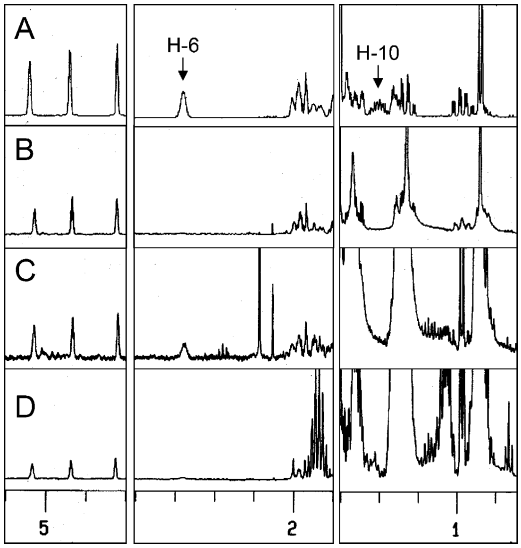

Figure 3. ^{1}H NMR spectra of amorphadienes: (A) authentic amorpha-4,11-diene; (B) from [1,1-$^2H_2$]farnesyl diphosphate; (C) from (1*S*)-[1-^{2}H]farnesyl diphosphate; (D) from (1*R*)- [1-^{2}H]farnesyl diphosphate.

labeling at H-6 and H-10. Collapse of the H-15 signal at δ 0.88 into a singlet further supported the labeling of H-10 with ^{2}H. In amorphadiene derived from (1*S*)-[1-^{2}H]farnesyl diphosphate, the characteristic H-10 signal at δ 1.40 disappeared (Figure 3C). On the other hand, the ^{1}H NMR spectrum of amorphadiene derived from (1*R*)-[1-^{2}H]farnesyl diphosphate was devoid of a H-6 signal at δ 2.55 (Figure 3D). These results unambiguously indicated that H_S-1 (H_a-1) of farnesyl diphosphate migrated to H-10 of amorphadiene, while H_R-1 (H_b-1) remained at its position to label amorphadiene H-6.

Deduction of Cyclization Mechanism. Brodelius' group proposed a cyclization mechanism of ADS based on the structure of ADS reaction byproducts; formation of compounds with a bisabolane skeleton such as α-bisabolol, *β*-sesquiphellandrene, and zingiberene as minor byproducts led to the proposal that the 1,6-closure involving a bisabolyl carbocation intermediate precedes the 1,10-closure (pathway a, Figure 1).[14,19] The group recently concluded that 1,6-ring closure is the first event and 1,3-hydride shift of the original H_S-1 of farnesyl diphosphate is operating in the ADS action,[15] based on the experiment involving farnesyl diphosphate asymmetrically labeled at C-1 with deuterium. Many sesquiterpene cyclases such as CDS from cotton are known to operate through the germacryl mechanism (pathway c, Figure 1).[11]

To establish the correct ADS mechanism from among the three possibilities (Figure 1), migration of farnesyl diphosphate H-1 during cyclization was traced using deuterium-labeled farnesyl diphosphates as substrate. The site of deuteration in the resulting labeled amorphadienes could be directly observed by ^{2}H NMR spectra of high signal-to-noise ratio (Figure 2). Even with only the labeling pattern of amorphadiene from [1,1-$^2H_2$]farnesyl diphosphate at hand, differentiation of the alternative mechanisms became possible. Retention of two deuterium atoms at C-1 of amorphadiene **6** easily eliminated pathway c from the possibilities, because, with pathway c in operation, one of the labels at farnesyl diphophate H-1 would migrate to amorphadiene C-11 through 1,3-shift (**7**, Figure 1) before being eliminated in the process of double-bond formation at the isopropenyl side chain.

Bisabolyl carbocation intermediate **3** (Figure 1, pathway a) arising from 1,6-closure would undergo hydride shift through either one direct suprafacial 1,3-shift of axial H_a-1 to C-7 (**4**, pathway a, Figure 1) or two suprafacial 1,2-hydride shifts, axial H_b-1 to C-6 and H-6 to C-7 (**4a**, pathway b), resulting in the correct *cis*-decalin configuration at C-1 and C-6 of **6**. Hence, only pathway a would result in amorphadiene with deuterium at C-6 and C-10. Stereochemical considerations also favor pathway a over b, because only the axial hydrogen atom is allowed to migrate in the process of suprafacial hydride shift; therefore, the ring conformation of intermediate **3** would dictate which hydrogen is to migrate. If the hydrogen atom H_a were in an axial orientation, allowing 1,3-hydride shift in the intermediate **4**, the side chain would be at an equatorial position (Figure 4). Model building demonstrated that this equatorial disposition of the side chain enabled the intermediate to fold into the appropriate conformation needed for the second ring closure. On the other hand, if H_b were to migrate via 1,2-hydride shift, the conformation of the intermediate **3a** would be such that H_b and the side chain point in the opposite axial directions. Molecular modeling showed that the axial conformation of the side chain in intermediate **4** is not favorable for the completion of the second ring closure by p-orbital overlap. Therefore, the final labeling pattern at H-1 and H-10 of amorphadiene derived from [1,1-$^2H_2$]farnesyl diphosphate enables differentiation between pathways a and b, with pathway a additionally supported by the conformational analysis of the putative reaction intermediates. Indeed, one of the labels was found at H-6 and another at H-10 in support of pathway a.

The above conclusion was supported through cryptochemistry of *pro-R* (H_b) and *pro-S* (H_a), H-1 hydrogens that gave direct support to the detailed cyclization mechanism (Figure 4). This work reconfirmed the stereochemical course of the reaction presented by Picaud et al., who also employed the chirally deuterated farnesyl diphosphate to probe the mechanism.[15] In the cyclization of farnesyl diphosphate, isomerization of farnesyl diphosphate into nerolidyl diphosphate (**2**, NDP) is a prerequisite for correct 1,6-ring closure. An alternative to the isomerization is the rotation of the C-2−C-3 bond after the formation of an allylic farnesyl cation−pyrophosphate anion ion pair, giving conformation **2** with H_b (*pro-R* H-1H_R of **1**) *cis* to the main chain. Attack of C-1 at the *si*-face of C-6 positions H_a-1 at the axial direction and the side chain in the desirable equatorial position of **3**. This axial disposition of H_a-1 enables suprafacial transfer of the hydrogen to the empty p-orbital at C-7 of **3**. The migration results in the *R* configuration at C-7 on **5**, which is the correct C-7 configuration of amorphadiene **6**. The migration of a hydrogen atom introduces the positive charge at C-1 with the p-orbital in the axial direction (**4**). The final ring closure between C-1 and C-10 in structure **4** leads to the desirable *cis*-decalin configuration in compound **6**, amorpha-4,11-diene.

Deuterium Exchange in ^2H_2O. Amorphadiene derived from the incubation of farnesyl diphosphate and ADS in deuterium oxide showed a molecular ion at *m*/*z* 205, which indicated the incorporation of one deuterium atom from the reaction medium (Supporting Information). The labeling pattern observed in the mass spectrum was indistinguishable from those of amorphadienes derived from singly labeled farnesyl diphosphates; therefore, the position of the label could not be determined through mass spectrometric analysis. The activity of ADS dramatically decreased when changing the medium from H_2O to ^2H_2O. Therefore, a large-scale preparation of amorphadiene in ^2H_2O for NMR analysis was not practical.

However, because amorphadiene obtained from deuterated farnesyl diphosphate retains the deuterium label at H-6 and H-10 in ^2H_2O, the position of deuterium exchange would not be H-6 or H-10. One of the possible mechanisms, though unprecedented, compatible with deuterium incorporation from the reaction medium is presented in Figure 4. In this mechanism, the intermediate **4** loses allylic H-6 to generate 2,6,10-bisabolatriene **8**, which would pick up one deuterium from the ^2H_2O medium on return. A large kinetic isotope effect is expected in the process. Indeed, deuterium incorporation was not observed in the medium even with up to 75% ^2H_2O.

Experimental Section

General Experimental Procedures. Protein concentration was determined using the Bio-Rad protein assay kit according to the

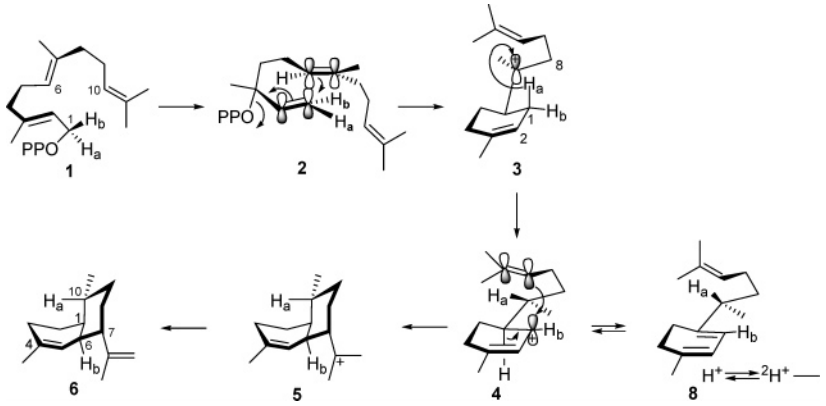

Figure 4. Cyclization mechanism of ADS.

manufacturer's instruction (Bulletin LIT33 REV C, Bio-Rad Laboratories) with bovine serum albumin (Sigma) as a standard. The electrophoresis with the standard molecular marker (Bio-Rad) was carried out through Laemmli's method using 10% polyacrylamide gel on a vertical slab gel electrophoresis apparatus (Hoefer). Electrophoresis run started at 75 V, and when the samples completely entered the stacking gel, the voltage was raised to 150 V. The gels were stained with 0.025% (w/v) Coomassie Brilliant Blue R-250 (Bio-Rad Laboratories) and destained with 10% MeOH and 10% HOAc solution. ^{1}H (400 MHz), ^{31}P (121 MHz), and ^{2}H (61.25 MHz) NMR spectra were recorded on a JEOL LA400 (JEOL, Japan). For measurement of ^{2}H NMR, $CDCl_3$ in $CHCl_3$ was used as a chemical shift standard. Before processing the data, 10 000 transients were accumulated to ensure proper signal-to-noise ratio. GC-MS analyses were performed on a Hewlett-Packard 5890 series II (Palo Alto, CA) using a DB-5 column (30 m × 0.25 μm × 0.25 mm) equipped with a JEOL AX505WA mass spectrometer (JEOL, Japan) operating in the electron impact mode at 70 eV. Separation conditions were as follows: injection port 200 °C, flame ionization detector 250 °C, split ratio 5:1, and helium flow 1.0 mL min^{-1}. Temperature program for the enzyme reaction product was as follows: 100 °C for 2 min, increase to 150 °C (5 °C min^{-1}), isothermal for 2 min, further increase to 250 °C (10 °C min^{-1}), and final isothermal for 2 min at 250 °C.

Synthesis of Deuterium-Labeled Farnesyl Diphosphates. The [1,1-$^{2}H_2$]farnesyl diphosphate, (1*R*)-[1-^{2}H]farnesyl diphosphate, and (1*S*)-[1-^{2}H]farnesyl diphosphate samples were synthesized according to the modified procedure of Benedict et al.[21] In short, farnesol was oxidized into farnesal by MnO_2 and reduced back to farnesol with $NaB^{2}H_4$. [1-^{2}H]-Farnesol was reoxidized to obtain [1-^{2}H]farnesal. High kinetic isotope effect ensured almost 100% deuterium retention on H-1. The labeled farnesal was subsequently reduced with $NaB^{2}H_4$ to give [1,1-$^{2}H_2$]-farnesol, or with (*R*)- and (*S*)-alpine-boranes yielding (1*S*)- and (1*R*)-[1-^{2}H]farnesol, respectively. Farnesol was chlorinated with *N*-chlorosuccinimide and finally pyrophosphorylated with tris(tetra-*n*-butyl) ammonium hydrogen pyrophosphate. The resulting farnesyl diphosphates were isolated by cellulose column chromatography and stored at −70 °C as ammonium salts before use. The synthesis of farnesyl diphosphates was verified through ^{1}H and ^{31}P NMR (data not shown).

Construction of Expression Plasmid. *E. coli* BL21(DE3)pLysS [hsdS, gal (λclts857, ind1, sam7, nin5, lacUV5-T7 gene1)] harboring KCS12 was used as an ADS source.[10] To isolate the ADS insert for cloning into pRSET A vector (Invitrogen), the plasmid was digested with *Bam*HI and *Eco*RI, and the digests were purified using the PCR purification kit (Takara). *Bam*HI and *Eco*RI-digested pRSET A were subjected to overnight ligation in the presence of T4 DNA ligase (Promega). The ligated samples, which contained a nucleotide sequence coding for six histidines placed upstream in frame with the pET-5a ADS insert, were transformed into BL21(DE3) cells. A single colony obtained on Luria-Bertani (LB)-ampicillin plates was selected and grown for use in the glycerol stocks, and the sequence of the plasmid was verified.

Bacterial Expression and Purification of His_6-Tagged ADS. BL21(DE3) cells, which harbored a plasmid containing the ADS insert, were grown overnight at 37 °C in 50 mL of LB broth supplemented with ampicillin (50 μg/mL). The preculture was used to inoculate 500 mL of LB medium containing ampicillin in a flask, and the cells were grown at 37 °C with continuous shaking until the optical density at 600 nm reached 0.5. At this point, isopropyl-β-D-thiogalactopyranoside (IPTG) was added to give a final concentration of 0.4 mM, and the culture was grown at 20 °C for an additional 6 h. The induced bacteria were harvested by centrifugation at 7000*g* on a Beckman Avanti 30 centrifuge at 4 °C for 10 min. The cell pellets were then frozen in liquid N_2 and stored at −70 °C. Prior to purification, bacterial pellets from 10 L culture were thawed and resuspended in 200 mL of lysis buffer (100 mM Tris-HCl, pH 8.0, 10% glycerol, 1 mM PMSF, 5 mM $MgCl_2$), and the suspension was incubated on ice for 30 min. The lysate was further homogenized by sonication with a 20 s pulse (VC-600, Fisher), and the homogenate was centrifuged at 10000*g* at 4 °C for 20 min. The resulting supernatant was applied to Ni-NTA resin (Invitrogen) that had been pre-equilibrated with the lysis buffer. The unbound proteins were eluted from the column using 150 mM imidazol in 10 bed volumes of the washing buffer (50 mM NaH_2PO_4, pH 7.0, 300 mM NaCl). All purification procedures were carried out at 4 °C. Protein content and SDS-PAGE pattern of the eluent were monitored to identify ADS fractions.

Amorpha-4,11-diene Production by ADS. ADS was used as tagged with histidine, because a preliminary experiment showed that the presence of the tag had little effect on the enzyme activity. The reaction mixture for amorpha-4,11-diene production contained 100 mg of purified ADS, 4 mM $MgCl_2$, 30 mM HEPES, pH 8.0, 3 mM β-mercaptoethanol, 4 mM DTT, and 100 μM farnesyl diphosphate in a total volume of 1 mL. Each reaction mixture was then covered with 1 mL of hexane, sealed with Parafilm, and incubated at 25 °C for 6 h. One hundred reactions were carried out for each farnesyl diphosphate. Subsequently, the reaction mixture was extracted three times with 100 mL of hexane. The combined hexane extract was passed through a silica gel column (1.5 cm × 5 mm i.d.) covered with anhydrous $MgSO_4$ (1 cm) to yield the terpene hydrocarbon fraction. The hexane extract was concentrated under nitrogen stream before GC-MS and NMR analyses. For the enzyme reaction in $^{2}H_2O$, the reaction medium without the enzyme was lyophilized and suspended in $^{2}H_2O$. The process was repeated to ensure complete exchange with deuterium. The enzyme was separately freeze-dried and resuspended in the reaction buffer before the initiation of the reaction.

Authentic Amorpha-4,11-diene. Amorpha-4,11-diene was synthesized through the reduction of artemisinic acid via artemisinol,[10] and the structure was confirmed through MS and NMR analyses for unambiguous assignment of NMR signals and found consistent with published data.[10,15]

Acknowledgment. This study was supported by the SRC program of MOST/KOSEF (R11-2000-081) through the Plant Metabolism Research Center, Kyung Hee University, and Brain Korea 21 Project administered by Ministry of Education and Human Resources, Korea. The measurement of deuterium spectra by Mr. P.-H. Kim, JEOL Korea, and critical reading of the manuscript by Dr. D. E. Cane are appreciated.

Supporting Information Available: SDS polyacrylamide gel electropherogram of ADS and mass spectra of the labeled amorpha-diene. This material is available free of charge via the Internet at http://pubs.acs.org.

References and Notes

(1) Flesch, G.; Rohmer, M. *Eur. J. Biochem.* **1988**, *175*, 405−411.
(2) Broers, S. T. J. Ph.D. Thesis, ETH, Zürich, 1994.
(3) Schwarz, M. K. Ph.D. Thesis, ETH, Zürich, 1994.
(4) Bohlmann, J.; Meyer-Gauen, G.; Croteau, R. *Proc. Natl. Acad. Sci. U.S.A.* **1998**, *95*, 4126−4133.
(5) Cane, D. E.; Pawlak, J. L.; Horak, R. M. *Biochemistry* **1990**, *29*, 5476−5490.
(6) Schmidt, C. O.; Bouwmeester, H. J.; Bulow, N.; Konig, W. A. *Arch. Biochem. Biophys.* **1999**, *364*, 167−177.
(7) He, X.; Cane, D. E. *J. Am. Chem. Soc.* **2004**, *126*, 2678−2679.
(8) Starks, C. M.; Back, K.; Noel, J. P.; Chappell, J. *Science* **1997**, *277*, 1815−1820.
(9) Klayman, D. L. *Science* **1985**, *228*, 1049−1055.
(10) Chang, Y. J.; Song, S. H.; Park, S. H.; Kim, S. U. *Arch. Biochem. Biophys.* **2000**, *383*, 178−184.
(11) Benedict, C. R.; Lu, J. L.; Pettigrew, D. W.; Liu, J.; Stipanovic, R. D.; Williams, H. J. *Plant Physiol.* **2001**, *125*, 1754−1765.
(12) Deligeorgopoulou, A.; Allemann, R. K. *Biochemistry* **2003**, *42*, 7741−7747.
(13) Cane, D. E.; Watt, R. M. *Proc. Natl. Acad. Sci. U.S.A.* **2003**, *100*, 1547−1551.
(14) Picaud, S.; Olofsson, L.; Brodelius, M.; Brodelius, P. E. *Arch. Biochem. Biophys.* **2005**, *436*, 215−226.
(15) Picaud, S.; Mercke, P.; He, X.; Sterner, O.; Brodelius, M.; Cane, D. E.; Brodelius, P. E. *Arch. Biochem. Biophys.* **2005**, published on web. DOI: 10.1016/j.abb.2005.07.015.
(16) Bohlmann, F.; Gerke, T.; Jakupovic, J.; King, R. M.; Robinson, H. *Phytochemistry* **1984**, *23*, 1183−1184.
(17) Midland, M. M.; Greer, S.; Tramontano, A.; Zderic, S. A. *J. Am. Chem. Soc.* **1979**, *101*, 2352−2355.
(18) Shibuya, M.; Chou, H. M.; Fountoulakis, M.; Hassam, S.; Kim, S. U.; Kobayashi, K.; Otsuka, H.; Rogalska, E.; Cassady, J. M.; Floss, H. G. *J. Am. Chem. Soc.* **1990**, *112*, 297−304.
(19) Mercke, P.; Bengtsson, M.; Bouwmeester, H. J.; Posthumus, M. A.; Brodelius, P. E. *Arch. Biochem. Biophys.* **2000**, *381*, 173−180.
(20) Chang, Y. J.; Jin, J.; Nam, H. Y.; Kim, S. U. *Biotechnol. Lett.* **2005**, *27*, 285−288.
(21) Benedict, C. R.; Alchanati, I.; Harvey, P. J.; Liu, J.; Stipanovic, R. D.; Bell, A. A. *Phytochemistry* **1995**, *39*, 327−331.

NP050356U